

Supporting Information

A Linear Trinuclear Ferrous Single Molecule Magnet

Shihao Liu,^{a,#} Yi-Fei Deng,^{a,#} Chang'An Li,^a Xiaoyong Chang^a and Yuan-Zhu Zhang^{*a}

^a Department of Chemistry, Southern University of Science and Technology, Shenzhen, 518055, P. R. China.

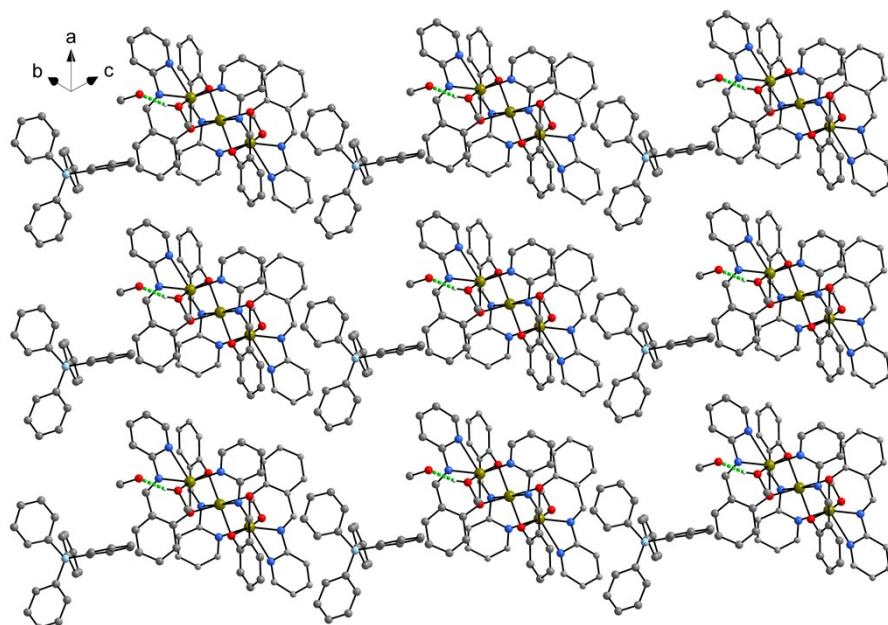


Figure S1. Packing view of **1** showing a 3D structure. Colour codes: dark yellow = Fe, red = O, grey = C, pale blue = B, blue = N.

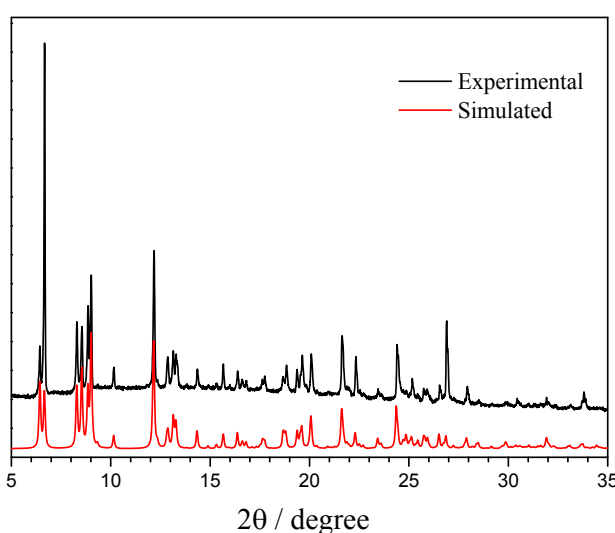


Figure S2. Experimental and simulated powder x-ray diffraction patterns of **1**.

Table S1. Crystallographic data for complex **1**.

1	
Formula	C ₁₀₀ H ₉₂ B ₂ Fe ₃ N ₈ O ₈
Molecular weight /g mol ⁻¹	1722.98
Crystal system	Triclinic
Space group	P-1
a, Å	11.5264(11)
b, Å	14.2406(14)
c, Å	15.0986(15)
α, deg	72.543(3)
β, deg	68.325(3)
γ, deg	69.161(3)
V, Å ³	2111.5(4)
Z	1
D _{cal} /g cm ⁻³	1.355
Temperature, K	150
2θ range/ ^o	2.05 to 27.56
completeness	99.7 %
residual map, e Å ⁻³	1.054/-0.729
Goodness-of-fit on F ²	1.111
Final indices[I > 2σ(I)]	R ₁ = 0.0625, wR ₂ = 0.1368
R indices (all data)	R ₁ = 0.0929, wR ₂ = 0.1524

Table S2. Selected Bond lengths [Å] and angles [deg] for **1**.

Fe(1)-O(1)	2.005(2)	O(1)-Fe(1)-O(2)#1	83.71(9)
Fe(1)-O(2)#1	2.194(2)	O(1)-Fe(1)-O(3)	97.70(10)
Fe(1)-O(3)	2.156(2)	O(1)-Fe(1)-N(1)	145.27(9)
Fe(1)-N(1)	2.437(3)	O(1)-Fe(1)-N(2)	86.22(10)
Fe(1)-N(2)	2.063(3)	O(1)-Fe(1)-N(3)	114.81(10)
Fe(1)-N(3)	2.126(3)	O(2)#1-Fe(1)-N(1)	98.24(9)
Fe(2)-O(1)	2.219(2)	O(3)-Fe(1)-O(2)#1	169.55(9)
Fe(2)-O(1)#1	2.220(2)	O(3)-Fe(1)-N(1)	86.53(10)
Fe(2)-O(2)	2.010(2)	N(2)-Fe(1)-O(2)#1	95.05(9)
Fe(2)-N(4)	2.161(3)	N(2)-Fe(1)-O(3)	95.38(10)
		N(2)-Fe(1)-N(1)	59.06(11)
		N(2)-Fe(1)-N(3)	157.71(11)
		N(3)-Fe(1)-O(2)#1	80.79(9)
		N(3)-Fe(1)-O(3)	89.27(10)
		N(3)-Fe(1)-N(1)	99.64(11)
		O(2)#1-Fe(2)-O(1)	82.93(8)
		O(2)-Fe(2)-O(1)	97.07(8)
		O(2)#1-Fe(2)-N(4)	92.64(9)
		O(2)-Fe(2)-N(4)	87.36(9)
		N(4)-Fe(2)-O(1)#1	93.13(9)
		N(4)-Fe(2)-O(1)	86.87(9)
		Fe(1)-O(1)-Fe(2)	91.05(8)
		Fe(2)-O(2)-Fe(1)#1	91.65(8)

Symmetry transformations used to generate equivalent atoms: #1 -x+1,-y,-z+1

Table S3. Parameters fitted by a generalized Debye model at 1200 Oe dc field.

T / K	τ / s	α
1.8	3.98×10^{-2}	0.243
2.0	2.68×10^{-2}	0.337
2.2	1.35×10^{-2}	0.266
2.4	7.12×10^{-3}	0.225
2.6	3.67×10^{-3}	0.193
2.8	1.89×10^{-3}	0.162
3.0	9.37×10^{-4}	0.139
3.2	4.67×10^{-4}	0.128
3.3	3.37×10^{-4}	0.122
3.4	2.46×10^{-4}	0.111
3.5	1.81×10^{-4}	0.101
3.6	1.33×10^{-4}	0.094
3.7	1.01×10^{-4}	0.081
3.8	7.90×10^{-5}	0.067
3.9	6.13×10^{-5}	0.056
4.0	4.65×10^{-5}	0.049

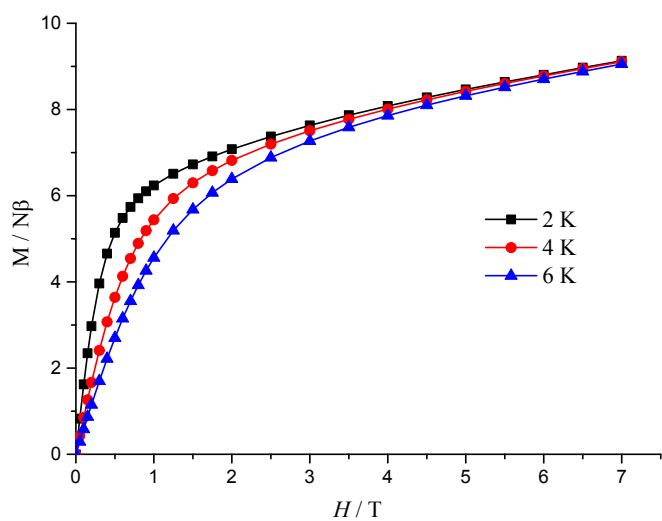


Figure S3. Field dependence of the magnetization (M) for **1** at 2-6 K. Solid lines are guides for the eyes.

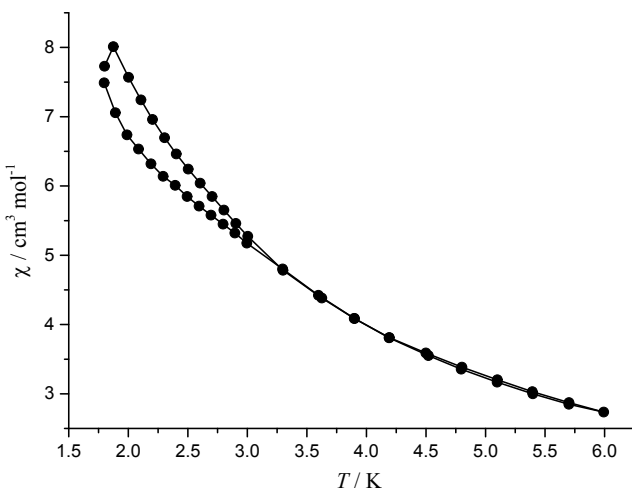


Figure S4. ZFC and FC magnetization versus temperature curves of **1** measured with applied field of 10 Oe. Solid lines are guides for the eyes.

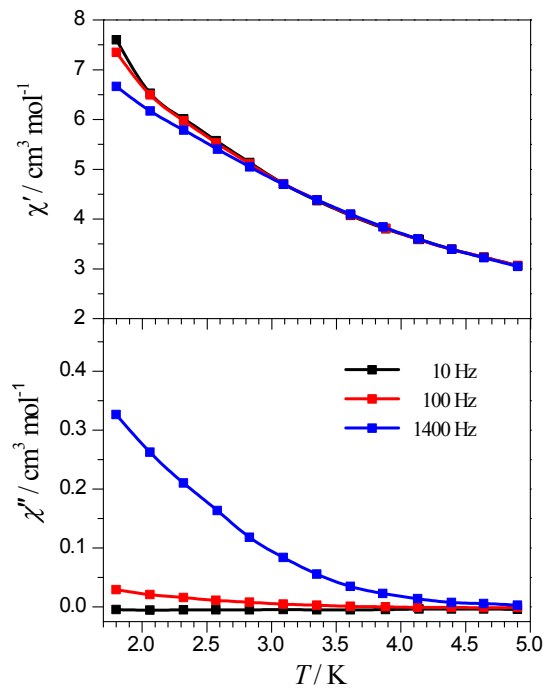


Figure S5. Temperature dependence of the in-phase (χ') and out-of-phase (χ'') ac susceptibility for **1** under zero dc field. The lines are guides to the eyes.

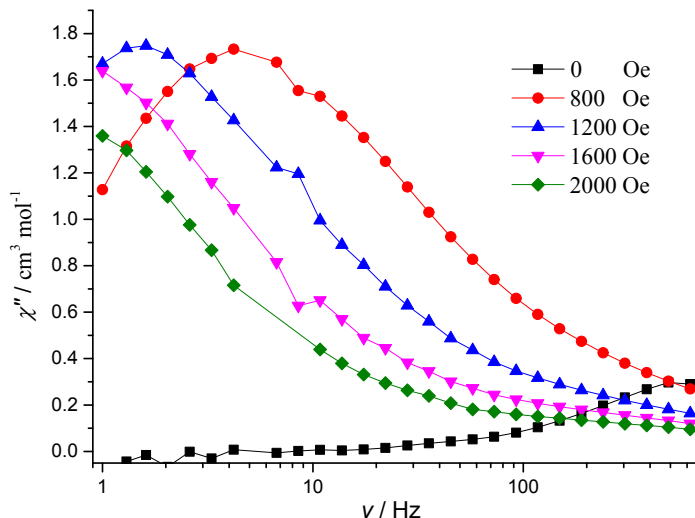


Figure S6. Variable-frequency out-of-phase (χ'') components of the ac magnetic susceptibility data for **1**, collected at temperatures of 2.0 K with 0-2000 Oe dc fields.

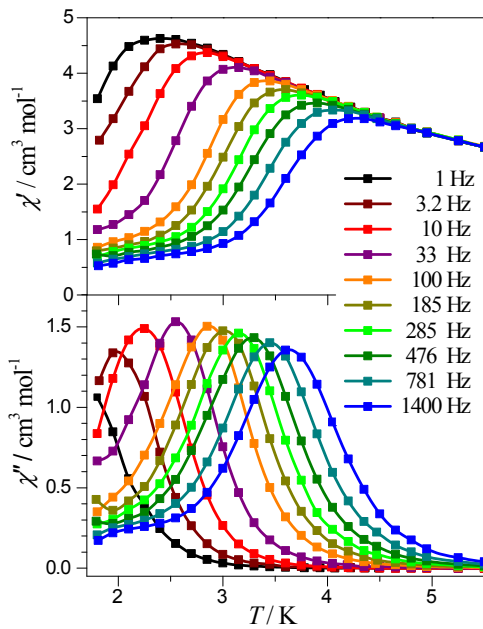


Figure S7. Temperature dependence of the in-phase (χ') and out-of-phase (χ'') ac susceptibility for **1** at 1200 Oe dc field. The lines are guides to the eyes.

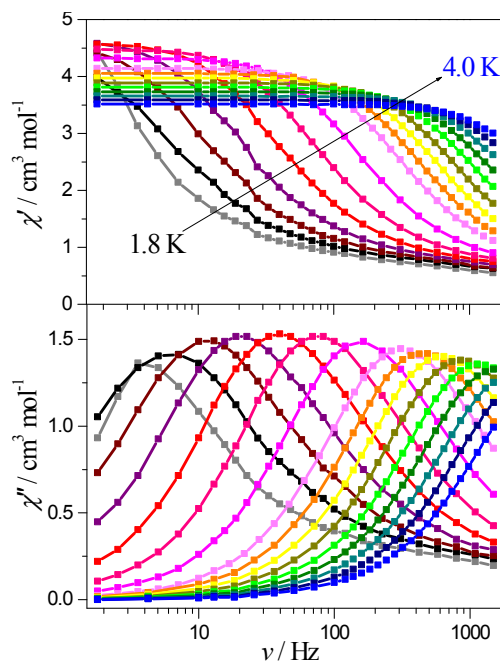


Figure S8. Frequency dependence of the in-phase χ' (top) and out-of-phase χ'' (bottom) components of the ac susceptibility for the complex **1** measured at 1200 Oe dc field. The lines are guides to the eyes.

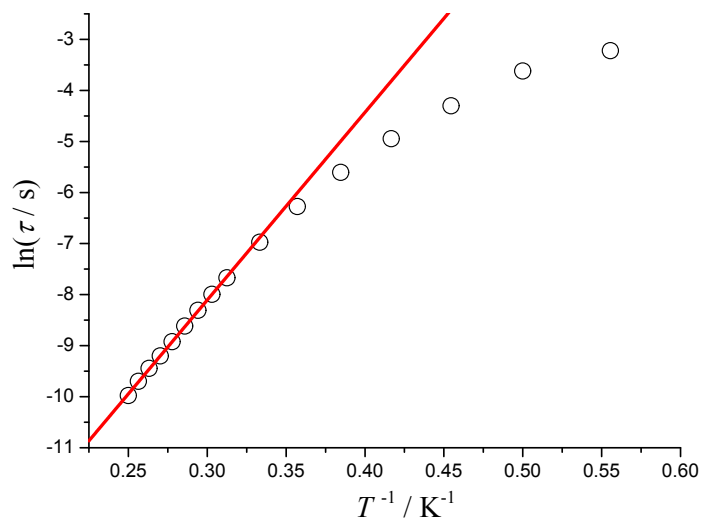


Figure S9. Temperature dependence of the relaxation rates for **1** under 1200 Oe dc field. The red line corresponds to the high-temperature Arrhenius fitting.